NASA/TM—2002-211153/PART1

Slow Crack Growth of Brittle Materials With Exponential Crack-Velocity Formulation—Part 1: Analysis

Sung R. Choi
Ohio Aerospace Institute, Brook Park, Ohio

Noel N. Nemeth and John P. Gyekenyesi
Glenn Research Center, Cleveland, Ohio

June 2002

The NASA STI Program Office . . . in Profile

Since its founding, NASA has been dedicated to the advancement of aeronautics and space science. The NASA Scientific and Technical Information (STI) Program Office plays a key part in helping NASA maintain this important role.

The NASA STI Program Office is operated by Langley Research Center, the Lead Center for NASA's scientific and technical information. The NASA STI Program Office provides access to the NASA STI Database, the largest collection of aeronautical and space science STI in the world. The Program Office is also NASA's institutional mechanism for disseminating the results of its research and development activities. These results are published by NASA in the NASA STI Report Series, which includes the following report types:

- TECHNICAL PUBLICATION. Reports of completed research or a major significant phase of research that present the results of NASA programs and include extensive data or theoretical analysis. Includes compilations of significant scientific and technical data and information deemed to be of continuing reference value. NASA's counterpart of peer-reviewed formal professional papers but has less stringent limitations on manuscript length and extent of graphic presentations.

- TECHNICAL MEMORANDUM. Scientific and technical findings that are preliminary or of specialized interest, e.g., quick release reports, working papers, and bibliographies that contain minimal annotation. Does not contain extensive analysis.

- CONTRACTOR REPORT. Scientific and technical findings by NASA-sponsored contractors and grantees.

- CONFERENCE PUBLICATION. Collected papers from scientific and technical conferences, symposia, seminars, or other meetings sponsored or cosponsored by NASA.

- SPECIAL PUBLICATION. Scientific, technical, or historical information from NASA programs, projects, and missions, often concerned with subjects having substantial public interest.

- TECHNICAL TRANSLATION. English-language translations of foreign scientific and technical material pertinent to NASA's mission.

Specialized services that complement the STI Program Office's diverse offerings include creating custom thesauri, building customized data bases, organizing and publishing research results . . . even providing videos.

For more information about the NASA STI Program Office, see the following:

- Access the NASA STI Program Home Page at ***http://www.sti.nasa.gov***

- E-mail your question via the Internet to help@sti.nasa.gov

- Fax your question to the NASA Access Help Desk at 301–621–0134

- Telephone the NASA Access Help Desk at 301–621–0390

- Write to:
  NASA Access Help Desk
  NASA Center for AeroSpace Information
  7121 Standard Drive
  Hanover, MD 21076

NASA/TM—2002-211153/PART1

Slow Crack Growth of Brittle Materials With Exponential Crack-Velocity Formulation—Part 1: Analysis

Sung R. Choi
Ohio Aerospace Institute, Brook Park, Ohio

Noel N. Nemeth and John P. Gyekenyesi
Glenn Research Center, Cleveland, Ohio

National Aeronautics and
Space Administration

Glenn Research Center

June 2002

This report is a formal draft or working paper, intended to solicit comments and ideas from a technical peer group.

The Aerospace Propulsion and Power Program at NASA Glenn Research Center sponsored this work.

Available from

NASA Center for Aerospace Information
7121 Standard Drive
Hanover, MD 21076

National Technical Information Service
5285 Port Royal Road
Springfield, VA 22100

Available electronically at http://gltrs.grc.nasa.gov/GLTRS

Slow Crack Growth of Brittle Materials With Exponential Crack-Velocity Formulation—Part 1: Analysis

Sung R. Choi
Ohio Aerospace Institute
Brook Park, Ohio 44142

Noel N. Nemeth and John P. Gyekenyesi
National Aeronautics and Space Administration
Glenn Research Center
Cleveland, Ohio 44135

Summary

Extensive slow-crack-growth (SCG) analysis was made using a primary exponential crack-velocity formulation under three widely used load configurations: constant stress rate, constant stress, and cyclic stress. Although the use of the exponential formulation in determining SCG parameters of a material requires somewhat inconvenient numerical procedures, the resulting solutions presented gave almost the same degree of simplicity in both data analysis and experiments as did the power-law formulation. However, the fact that the inert strength of a material should be known in advance to determine the corresponding SCG parameters was a major drawback of the exponential formulation as compared with the power-law formulation.

Introduction

Advanced ceramics are candidate materials for structural applications in advanced heat engines and heat recovery systems. The major limitation of these materials in hostile environments, particularly at elevated temperatures, is slow-crack-growth (SCG)-associated failure, where slow crack growth of inherent defects or flaws can occur until a critical size for catastrophic failure is reached. To ensure accurate life prediction of ceramic components, it is important to accurately evaluate the SCG parameters of a material with specified loading and environmental conditions.

Life prediction (or SCG) parameters of a material depend on what type of crack-velocity formulation is used to determine them. The power-law crack-velocity formulation has been used for several decades to describe SCG behavior of a variety of brittle materials ranging from glass and glass ceramics to advanced structural ceramics. The main advantage of the power-law formulation over other crack-velocity formulations lies in the simplicity in its mathematical expression for lifetime analysis. It has also been observed that the power-law formulation has described adequately the SCG behavior of many brittle materials. Because of these merits, the power-law formulation has been used in two recent ASTM test standards (refs. 1 and 2) to determine SCG parameters of advanced ceramics in constant stress rate testing at both ambient and elevated temperatures. Alternative crack-velocity formulations take exponential forms to account for the influence of other phenomena (such as a corrosion reaction, diffusion control, thermal activation, etc.). However, these exponential forms generally do not result in simple mathematical expressions of life prediction formulation, although the forms might better represent the actual SCG behavior of some materials. Because of this mathematical inconvenience, the exponential crack-velocity formulation has rarely been used for brittle materials as a means of life prediction methodology in testing or analysis.

In this report, the exponential crack-velocity formulation was analyzed to achieve a more convenient and simplified life prediction analysis compared with the previous exponential crack-velocity-based analyses. The numerical analysis presented here was made for three widely utilized load configurations: constant stress rate (dynamic fatigue), constant stress (static fatigue or stress rupture), and cyclic stress (cyclic fatigue). The resulting analysis obtained with the exponential formulation was compared with that of the power-law formulation to assess which would yield a better life prediction methodology in terms of accuracy and convenience in testing and analysis. To the authors' best knowledge, no analytical study on slow crack growth has been done previously using the exponential formulation under cyclic loading. In the following reports (parts 2 and 3 of this series) the merits and limitations of the exponential formulation will be further described in detail using a variety of SCG data determined for many glasses and advanced ceramics at both ambient and elevated temperatures.

All symbols used in this report are listed in the appendix.

This work was sponsored in part by the HOT/PC and the ZCET projects at the NASA Glenn Research Center, Cleveland, Ohio.

Theoretical Background

Power-Law Formulation

The widely utilized empirical power-law crack-velocity term for above the fatigue limit is expressed in the form (ref. 3)

$$v = \frac{da}{dt} = A\left(\frac{K_I}{K_{IC}}\right)^n \tag{1}$$

where

v	crack velocity
a	crack size
t	time
K_I	mode I stress intensity factor
K_{IC}	mode I critical stress intensity factor (or fracture toughness)
A, n	material- and environment-dependent SCG parameters

Typically, SCG testing to determine related SCG parameters is performed by applying constant stress rate, constant stress, or cyclic stress loading to ground-test specimens. Constant stress rate testing determines strength as a function of applied stress rate, whereas constant stress and cyclic stress testing measure time to failure as a function of applied stress. The strength in constant stress rate and the time to failure in constant stress and cyclic stress tests can be analytically derived to give the following relations (refs. 4 and 5):

$$\sigma_f = D_d \dot{\sigma}^{1/(n+1)} \tag{2}$$

$$t_{fs} = D_s \sigma^{-n} \tag{3}$$

$$t_{fc} = D_c \sigma_{\max}^{-n} \tag{4}$$

where σ_f is the fracture stress corresponding to the applied stress rate $\dot{\sigma}$ in constant stress rate testing, t_{fs} is the time to failure subjected to a constant applied stress σ in constant stress testing, and t_{fc} is the time to failure subjected to cyclic loading with a maximum stress $\sigma_{\max}$ in cyclic stress testing. The parameters represented by D's are expressed as follows (refs. 4 and 5):

$$D_d = \left[B(n+1) S_i^{n-2} \right]^{1/(n+1)} \tag{5}$$

$$D_s = B S_i^{n-2} \tag{6}$$

$$D_c = \frac{\left(B S_i^{n-2} \right)}{\left\{ \frac{1}{\tau} \int_0^{\tau} \left[f(t) \right]^n \mathrm{d}t \right\}} \tag{7}$$

where $B = 2K_{IC}/[AY^2(n-2)]$ where Y is the crack geometry factor in the relation $K_I = Y\sigma a^{1/2}$; S_i is the inert strength at which no slow crack growth occurs; the function $f(t)$ is a periodic function in cyclic loading specified in $\sigma(t) = \sigma_{\max} f(t)$ in a range of $0 \le f(t) \le 1$; and τ is the period. The SCG parameters n and D (and B or A) can be obtained by a linear regression analysis with experimental data in conjunction with the corresponding equation, either (2), (3), or (4), depending on the type of loading. Hence, it is straightforward to determine SCG parameters n and D by least-squares fitting of the data, which is the most advantageous feature of the power-law crack-velocity formulation. This convenience and merit in mathematical simplicity in addition to the use of routine test techniques have led for several decades to the almost exclusive use of the power-law crack-velocity formulation in life prediction analysis and testing for many brittle materials over a wide range of temperatures.

Exponential Formulation

Fracture-mechanics-based modeling typically offers a framework in which lifing can be made. However, long-term life prediction is sensitive to the relation between the slow crack velocity and the stress intensity factor, which depends on many factors itself. As a result, several different exponential crack-velocity formulations that have been previously proposed are based on these other factors, which include the presence of a chemically assisted corrosion reaction (ref. 6), diffusion-controlled stress rupture (ref. 7), a thermally activated process (ref. 8), a chemical reaction with constant crack-tip configuration (ref. 9), kinetic crack growth (ref. 10), and others (ref. 11). The generalized exponential crack-velocity forms thus proposed are

$$v = A \exp\left[n \left(\frac{K_I}{K_{IC}} \right) \right] \tag{8}$$

$$v = A \left(\frac{K_I}{K_{IC}} \right) \exp\left[n \left(\frac{K_I}{K_{IC}} \right) \right] \tag{9}$$

$$v = A\left(\frac{K_{IC}}{K_I}\right)\exp\left[n\left(\frac{K_I}{K_{IC}}\right)\right] \tag{10}$$

$$v = A\exp\left[n\left(\frac{K_I}{K_{IC}}\right)^2\right] \tag{11}$$

$$v = A\left(\frac{K_I}{K_{IC}}\right)\exp\left[n\left(\frac{K_I}{K_{IC}}\right)^2\right] \tag{12}$$

where A and n are SCG parameters and are different from those used in the power-law formulation. Unlike the power-law crack-velocity formulation, the exponential crack-velocity forms do not yield simple, analytical expressions of either the resulting strength as a function of applied stress rate in constant stress rate testing or of the resulting time to failure as a function of applied stress in constant stress testing or maximum applied stress in cyclic stress testing. Several attempts have been made under both constant stress rate and constant stress loading to obtain corresponding lifetime expressions through numerical integration incorporating linear (refs. 12 and 13) or nonlinear (ref. 14) regression analysis. However, this approach still involves complexity in regression technique as compared with the simple least-squares approach in the power-law formulation.

Slow-crack-growth analyses of three load configurations of constant stress rate, constant stress, and cyclic stress were made in this section to obtain simpler, representative equations through numerical solution, which in turn makes the use of regression analysis easier to determine corresponding SCG parameters comparable to the case of the power-law formulation. Trantina (ref. 12) used the exponential crack-velocity forms (eqs. (8) to (10)) to determine the approximate time-to-failure equations under constant stress rate and constant stress loading and showed that the coefficients of the exponential equations (8) to (10) were insignificant except at very low fracture stress. Ritter et al. (ref. 13) used the exponential form (eq. (8)) to determine the relation of strength versus stress rate in constant stress rate loading via a numerical method for indentation cracks that possess a residual stress field around the indent. For the purpose of simplicity and generalization, equation (8) was chosen for the present analysis. This equation was taken from Wiederhorn and Bolz (ref. 9), who modified the original Hillig and Charles (ref. 6) exponential formulation. An additional analysis using other crack-velocity forms (eqs. (9) to (11)) was also made and the results will be discussed in the section Other Exponential Formulations.

To minimize the number of parameters to be specified (such as A, a, σ, S_i, K_{IC}, and t), it is convenient to use a normalized scheme, as used previously for the power-law velocity formulation (refs. 15 to 17):

$$K^* = \frac{K_I}{K_{IC}};\quad T^* = \frac{A}{a_i}t;\quad C^* = \frac{a}{a_i};\quad \sigma^* = \frac{\sigma}{S_i};\quad \dot{\sigma}^* = \frac{\sigma^*}{T^*};\quad \sigma^*_{\max} = \frac{\sigma_{\max}}{S_i} \tag{13}$$

where

K^* stress intensity factor (SIF)
T^* time
C^* crack size

σ^* applied stress
$\dot{\sigma}^*$ applied stress rate
σ^*_{max} maximum applied stress

in cyclic loading, and a_i is the critical crack size in the inert condition or is the initial crack size. Using these variables, the exponential crack-velocity equation (8) can be normalized as follows:

$$\frac{dC^*}{dT^*} = e^{nK^*} \tag{14}$$

The corresponding normalized SIF K^* is expressed in load configurations of constant stress rate, constant stress, and cyclic sinusoidal stress, respectively, as

$$K^* = \dot{\sigma}^* T^* \left(C^*\right)^{1/2} \tag{15}$$

$$K^* = \sigma^* \left(C^*\right)^{1/2} \tag{16}$$

$$K^* = \left\{\frac{1+R}{2} + \frac{1-R}{2}\sin\left[\left(\frac{\omega a_i}{A}\right)T^*\right]\right\}\sigma^*_{max}\left(C^*\right)^{1/2} \tag{17}$$

where R is the stress (or load) ratio, defined as $R = \sigma_{min}/\sigma_{max}$, in which σ_{min} and σ_{max} are the minimum and maximum applied stresses, respectively, applied in cyclic loading; and ω is the angular velocity. As typical for ceramics, the crack size at instability in either an inert or fatigue environment was assumed to be small compared with the body of the specimens or components (i.e., an infinite-body assumption). Differential equation (14) was solved numerically using a fourth-order Runge-Kutta method for each respective loading configuration. The initial condition was $C^* = 1.0$ at $T^* = 0$, and the instability conditions were $K^* = 1.0$ and $dK^*/dC^* > 0$. In cyclic loading, the frequency was taken as arbitrary values of $\omega a_i/A \geq 10^8$, depending on the values of maximum applied stress and n. The effect of frequency on the solution is discussed in the section Cyclic Stress Loading.

Results of Numerical Analysis

Constant Stress Rate Loading

The results of the numerical solution of normalized fracture stress (strength) σ^*_f as a function of normalized stress rate $\dot{\sigma}^*$ are shown in figure 1 for values of n ranging from 5 to 100. As seen in the figure, for a given n, strength decreases with decreasing stress rate and represents the susceptibility to slow crack growth. The rate of decrease in strength with decreasing stress rate becomes more significant with lower n values, analogous to the case for the power-law formulation, indicating that the lower n gives rise to the greater SCG susceptibility and vice versa. The strength approaches its corresponding inert strength as stress rate increases to a certain value at which no slow crack growth occurs. Likewise, the strength converges close to zero as the stress rate approaches $\ln \dot{\sigma}^* = 0$. A linear relationship between σ^*_f and $\ln \dot{\sigma}^*$ holds for most of n values within the range of $\sigma^*_f = 0.2$ to 0.9 with correlation coefficients of $r^2 \geq 0.9975$.

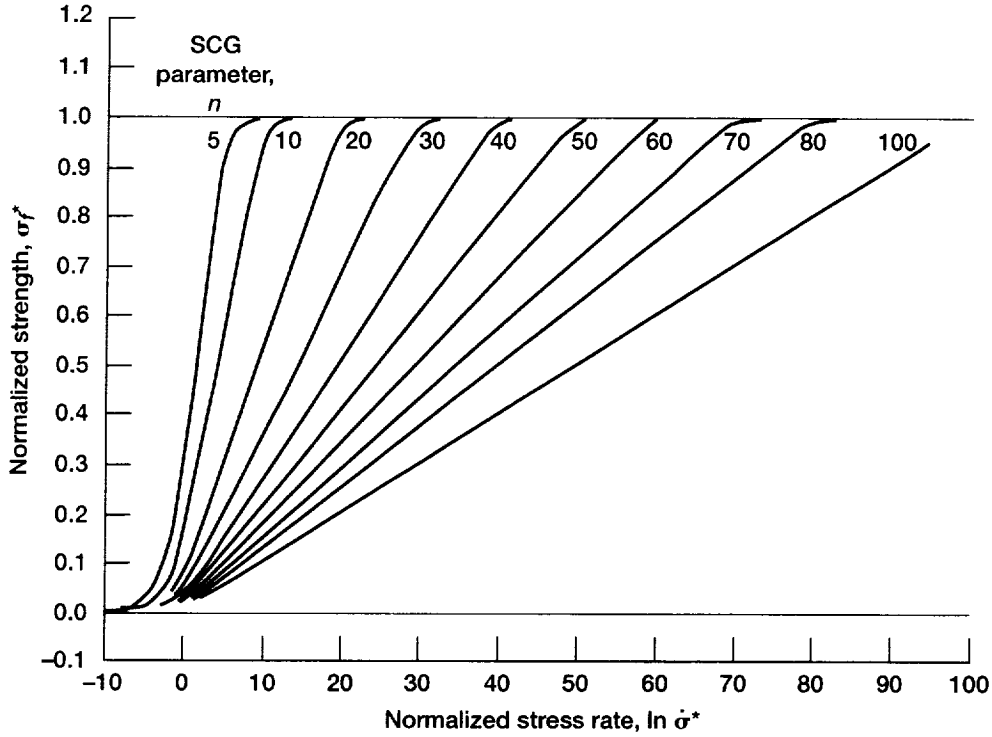

Figure 1.—Numerical results of normalized strength σ_f^* as a function of normalized stress rate $\dot{\sigma}^*$ in constant stress rate loading for different values of SCG parameter n.

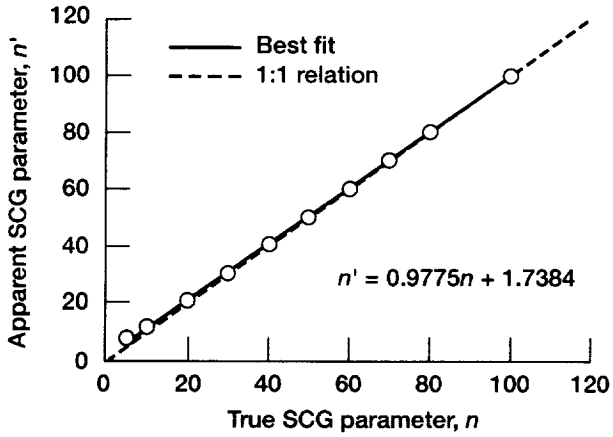

Figure 2.—Relationship between true SCG parameter n and apparent SCG parameter n' in constant stress rate loading.

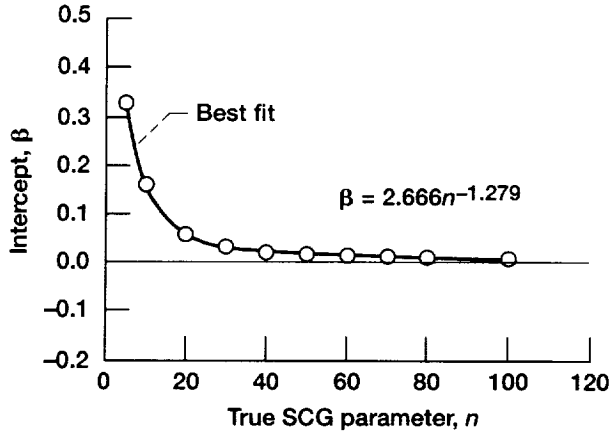

Figure 3.—Relationship between intercept β and true SCG parameter n in constant stress rate loading.

A linear regression analysis of σ_f^* and $\ln \dot{\sigma}^*$ in the range of $\sigma_f^* = 0.2$ to 0.9 was made to determine the slope and intercept of each individual curve for a given n, based on the following relation:

$$\sigma_f^* = \frac{1}{n'} \ln \dot{\sigma}^* + \beta \tag{18}$$

where $1/n'$ and β are the slope and intercept, respectively. A comparison of the true n (an input datum) and the apparent n' (calculated) is shown in figure 2, where a linear relationship between n and n' is evident (except for lower n values, particularly for $n < 10$). Hence, the overall relationship between n and n' can be approximated as

$$n' = 0.9775n + 1.7384 \tag{19}$$

with a correlation coefficient $r^2 = 0.9995$. Since the difference between n' and n was ≥8 percent for $n \leq 10$ and ≤3 percent for $n \geq 20$, a further approximation of equation (19) can be made for $n \geq 20$ as follows:

$$n' \approx n \tag{20}$$

The relationship between the intercept β and n is shown in figure 3. The value of β decreases with increasing n and becomes insignificant, approaching zero, when $n > 20$. The overall relationship between β and n in the range of $n = 5$ to 100 was

$$\beta = 2.666(n)^{-1.279} \tag{21}$$

with a correlation coefficient $r^2 = 0.9973$. For a nonnormalized expression, equation (13) is used to reduce equation (18) to

$$\frac{\sigma_f}{S_i} = \frac{1}{n'} \ln \dot{\sigma} + \chi \tag{22}$$

where

$$\chi = \frac{1}{n'} \ln\left(\frac{a_i}{AS_i}\right) + \beta \tag{23}$$

SCG parameters n' and χ in constant stress rate loading can be obtained from the slope and intercept by a linear regression analysis of (σ_f/S_i) versus $\ln \dot{\sigma}$. With n' thus calculated, n can be evaluated from equation (19). The parameter A can be evaluated using equation (23) from calculated χ together with β (eq. (21)) and known values of a_i and S_i. The solution presented in this study (eq. (22)) is much simpler compared with the previous solution by Trantina (ref. 12) in which a simple linear regression would hardly be applicable because of the complex functional form of the solution, as shown below (note that σ_f is present in both sides of the equation):

$$\frac{\sigma_f}{S_i} = \frac{1}{n} \ln \dot{\sigma} + \frac{1}{n} \ln\left[\left(\frac{2a_i}{A}\right)\sigma_f\right] \tag{24}$$

Therefore, when determining SCG parameters, the current solution (eq. (22)) significantly eliminates the complexity associated with a regression analysis that would be encountered in the previous solution (eq. (24)). For the case of $n > 20$, based on the results of figures 1 and 3 for $\sigma_f^* \geq 0.4$, β is negligible (with a maximum of about 7 percent) compared with σ_f^*. Hence, equation (21) reduces to

$$\beta \approx 0 \tag{25}$$

which results in $\chi \approx [\ln (a_i/AS_i)]/n$. Likewise, in this case, $n' \approx n$ from equation (20).

A distinct difference in functional expression between the power-law and exponential formulations is that in the power-law formulation, $\log \sigma_f$ is plotted as a function of $\log \dot{\sigma}$, whereas in the exponential formulation, σ_f/S_i is plotted as a function of $\ln \dot{\sigma}$ (fig. 1 shows this for the normalized parameters, σ_f^* as a function of $\ln \dot{\sigma}^*$). Hence, the knowledge of inert strength in the exponential formulation is a prerequisite to determining SCG parameters n' and χ, which is a disadvantage compared with the case (eq. (2)) of the power-law formulation. Note that the power-law formulation does not require any prior knowledge of inert strength to determine SCG parameters n and D. Although not presented here, the numerical result was plotted as $\log \sigma_f$ as a function of $\log \dot{\sigma}$ for different n values in the same way that is used for the power-law formulation. The resulting plots, however, showed appreciable nonlinearity, which made linear least-squares fitting inapplicable in determining the related SCG parameters.

Constant Stress Loading

The numerical results of normalized time to failure T_f^* as a function of normalized applied stress σ^* are shown in figure 4 for values of n ranging from 5 to 100. The general trend of the solution can be summarized in terms of (1) the convergence of $\ln T_f^*$ close to zero with $\sigma^* \to 0$, (2) the increased SCG susceptibility with decreasing n values, and (3) the linearity between $\ln T_f^*$ and σ^* in the range of $\sigma^* = 0.2$ to 0.9. As a consequence, the relationship between normalized time to failure and normalized applied stress within the linear region can be written as

$$\ln T_f^* = -n'\sigma^* + \beta \tag{26}$$

The linearity between $\ln T_f^*$ and σ^* is manifest when the correlation coefficient $r^2 \geq 0.995$ for each curve is considered. Hence, n' and β can be determined with a reasonable accuracy by a linear regression analysis based on the results in equation (26). The relationship between n' and n is shown in figure 5 and has the following relation:

$$n' = 0.9827n + 3.3440 \tag{27}$$

with $r^2 = 0.9997$. The difference between n' and n was ≥8 percent for $n \leq 30$ and ≤5 percent for $n \geq 40$ so that a further approximation of equation (27) can be made for the case of $n \geq 40$ as

$$n' \approx n \tag{28}$$

The function of β with respect to n is depicted in figure 6, where the intercept β decreases with increasing n values, resulting in the best-fit relation

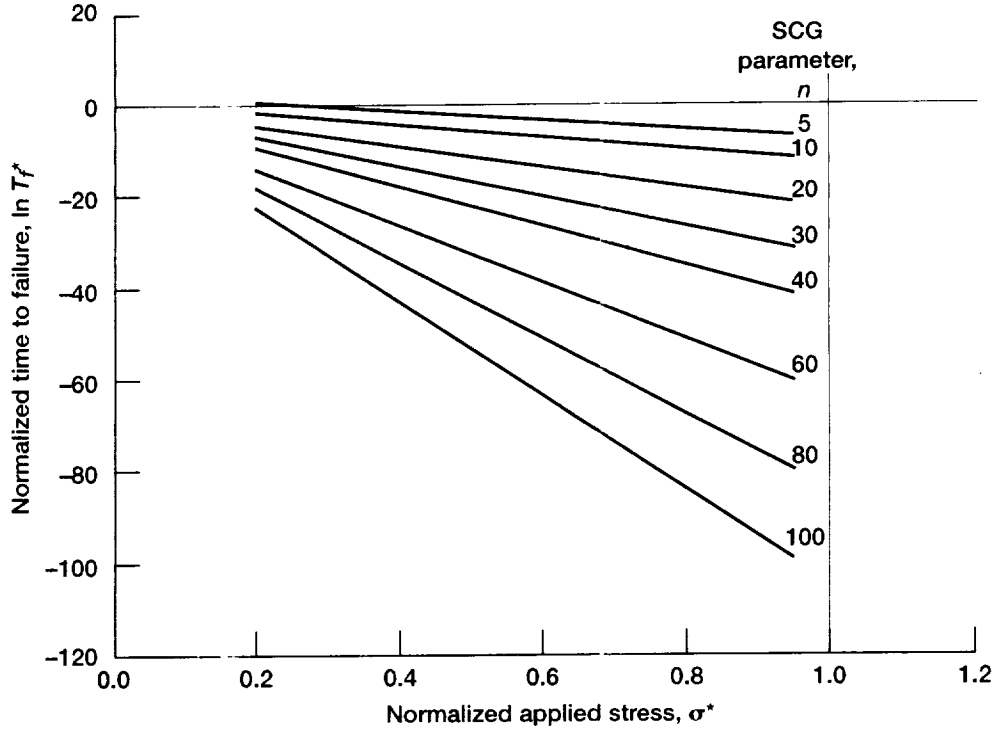

Figure 4.—Numerical results of normalized time to failure T_f^* as function of normalized applied stress σ^* in constant stress loading for different values of SCG parameter n.

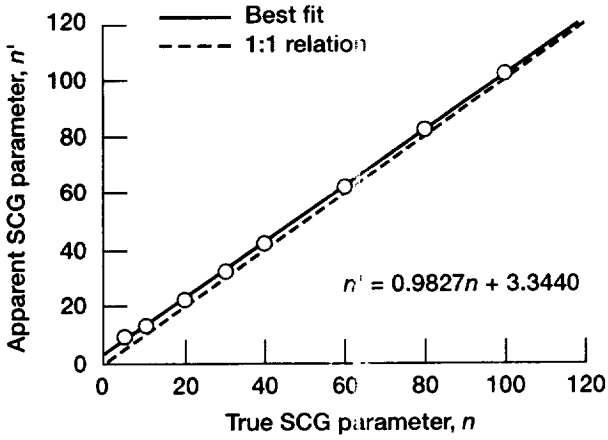

Figure 5.—Relationship between true SCG parameter n and apparent SCG parameter n' in constant stress loading.

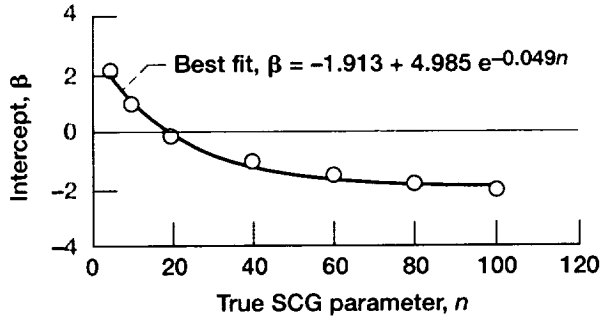

Figure 6.—Relationship between intercept β and true SCG parameter n in constant stress loading.

$$\beta = -1.913 + 4.985e^{-0.049n} \tag{29}$$

with $r^2 = 0.9907$.

For the nonnormalized expression, equation (13) is used to reduce equation (26) to

$$\ln t_f = -n' \frac{\sigma}{S_i} + \chi \tag{30}$$

where

$$\chi = \ln\left(\frac{a_i}{A}\right) + \beta \tag{31}$$

Hence, n' and χ in constant stress loading can be obtained from the slope and intercept, respectively, by a simple linear regression analysis of the data $\ln t_f$ as a function of σ/S_i. With n' calculated, n can be evaluated from equation (27). The parameter A can be estimated from equation (31) with calculated χ together with β (eq. (29)) and known values of a_i. The solution presented here is much simpler than the rather complex one proposed by Trantina (ref. 12), in which the slope of the relation $\ln t_f$ versus σ/S_i was $n + (S_i/\sigma)$. Both analyses, however, would give a similar result when n is significantly greater than S_i/σ.

A notable difference in constant stress loading analysis between the power-law and exponential formulations is that in the power-law formulation, $\log t_f$ is plotted as a function of $\log \sigma$ as seen in equation (3). However, in the exponential formulation, $\ln t_f$ is plotted as a function of σ/S_i. Hence, as in the case of constant stress rate loading, inert strength must be known to determine n' and χ, which is a distinctive drawback of the exponential formulation as compared with the power-law formulation. Unlike the power-law formulation (eq. (3)), there was significant nonlinearity in plots of $\log T_f^*$ as a function of $\log \sigma^*$ (not shown here), which made linear least-squares fitting inapplicable to determine the related SCG parameters.

Cyclic Stress Loading

The results of the numerical solution of normalized time to failure T_f^* as a function of normalized maximum applied stress σ_{max}^* in cyclic sinusoidal loading with two stress ratios R of 0.1 and 0.5 are shown in figure 7 for values of n ranging from 5 to 80. Similar to the case of constant stress loading, this plot is linear with respect to σ_{max}^* in the range 0.2 to 0.9 and converges close to zero with a further decrease in σ_{max}^*. The linearity between $\ln T_f^*$ and σ_{max}^* was evident considering the correlation coefficient of $r^2 \geq 0.997$. Also, note that the effect of the R-ratio on the solution for a given n value is insignificant. Based on the results in figure 7, similar to the case of constant stress loading, the relationship between $\ln T_f^*$ and σ_{max}^* can be described as follows:

$$\ln T_f^* = -n' \sigma_{max}^* + \beta \tag{32}$$

where n' is the slope and β is the intercept, which can be determined from the numerical results using a linear regression analysis based on equation (32).

Figure 8 shows the relationship between n' and n for R-ratios of 0.1 and 0.5. For comparison, the result determined in constant stress loading (i.e., $R = 1.0$) from figure 5 was also included. Note that the SCG analysis in cyclic stress loading reduces to that of constant stress loading when $R = 1.0$ (also seen in

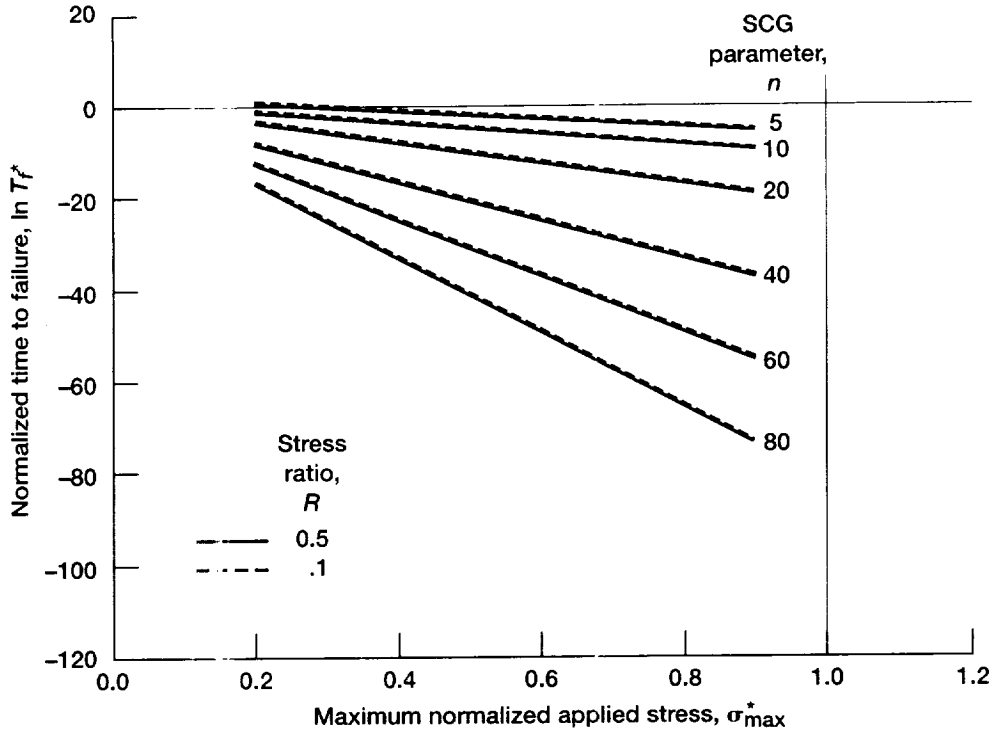

Figure 7.—Numerical results of normalized time to failure T_f^* as function of maximum normalized applied stress σ^*_{max} in cyclic (sinusoidal) stress loading for R-ratios of 0.1 and 0.5 and different values of SCG parameter n.

eq. (17)); hence, constant stress loading can be regarded as one of the generalized cyclic loading configurations. A good linear relation between n' and n was found for both $R = 0.1$ and 0.5 with $r^2 > 0.999$:

$$n' = 0.9777n + 2.5296 \quad \text{for } R = 0.1$$
$$n' = 0.9772n + 2.5411 \quad \text{for } R = 0.5 \tag{33}$$

As seen in figure 8, no significant difference in the n'-n relation exists for R-ratios ranging from 0.1 to 1.0 (constant stress loading): this relationship is also observed in the power-law formulation (refs. 5, 17, and 18). The difference between n' and n was ≥7 percent for $n \leq 20$ and ≤3 percent for $n \geq 40$, so that a further approximation of equation (33) can be made for $R = 0.1$ and 0.5 for the case of $n \geq 40$ as follows:

$$n' \approx n \tag{34}$$

The relationship between the intercept β and n is depicted in figure 9, where the result from figure 6 for constant stress loading ($R = 1.0$) was also included for comparison. The intercepts for $R = 0.1$ and 0.5 decrease more monotonically with increasing n values than that of $R = 1.0$. The best-fit equation, similar to equation (29) in constant stress loading, was obtained for each R-ratio:

$$\beta = 0.1409 + 3.559e^{-0.0737n} \quad \text{for } R = 0.1$$
$$\beta = 0.1182 + 3.782e^{-0.0857n} \quad \text{for } R = 0.5 \tag{35}$$

with the correlation coefficient of $r^2 \geq 0.991$.

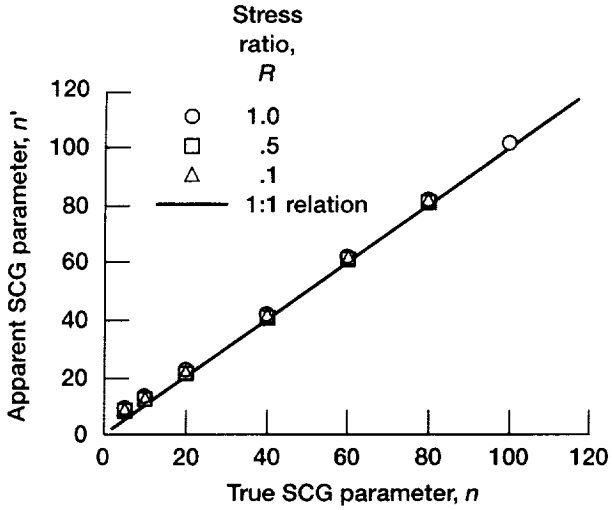

Figure 8.—Relationship between true SCG parameter n and apparent SCG parameter n' in cyclic (sinusoidal) stress loading with R-ratios of 0.1, 0.5, and 1.0.

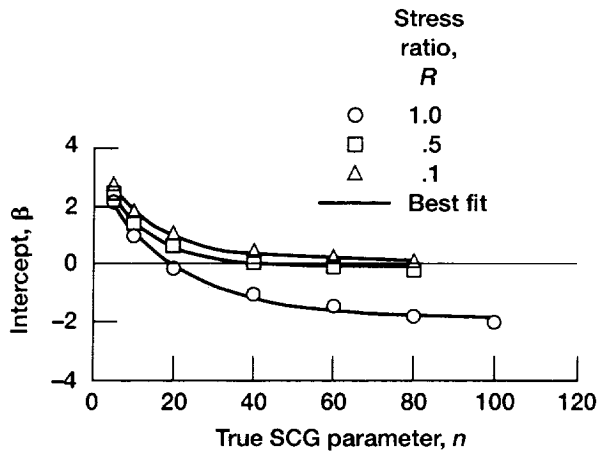

Figure 9.—Relationship between intercept β and true SCG parameter n in cyclic (sinusoidal) stress loading with R-ratios of 0.1, 0.5, and 1.0.

For the nonnormalized expression, equation (13) can be used to reduce equation (32) to

$$\ln t_f = -n' \frac{\sigma_{max}}{S_i} + \chi \tag{36}$$

where

$$\chi = \ln\left(\frac{a_i}{A}\right) + \beta \tag{37}$$

Therefore, n' and χ of the exponential formulation in cyclic stress loading for a given R-ratio can be obtained from the slope and intercept by a linear regression analysis of the data of $\ln t_f$ as a function of σ_{max}/S_i. With n' calculated, n can be evaluated from equation (33). The SCG parameter A can be estimated from equation (37) with calculated χ, β (eq. (35)), and known values of a_i.

In cyclic stress loading, a distinct difference between the power-law and exponential formulations is that in the power-law formulation, $\log t_f$ is plotted as a function of $\log \sigma_{max}$ as seen in equation (4) whereas in the exponential formulation, $\ln t_f$ is plotted as a function of σ_{max}/S_i. Hence, as in the cases of constant stress rate and constant stress loading, the inert strength of a material must be known in advance for cyclic loading to determine the corresponding SCG parameters, a clear disadvantage of the exponential formulation compared with the power-law formulation. Although not presented here, it was found that in plots of $\log T_f^*$ as a function of $\log \sigma_{max}^*$, typical of the power-law formulation (eq. (4)), there was a considerable nonlinearity that made linear least-squares fitting inapplicable in determining the related SCG parameters.

Typical examples of the effect of frequency on the time to failure in cyclic stress loading are shown in figure 10 for R-ratios of 0.1 and 0.5 with $n = 20$ and $\sigma_{max}^* = 0.9$. The number of cycles to failure N_f is calculated using the relation

$$N_f = \frac{T_f^*}{2\pi}\left(\frac{\omega a_i}{A}\right) \tag{38}$$

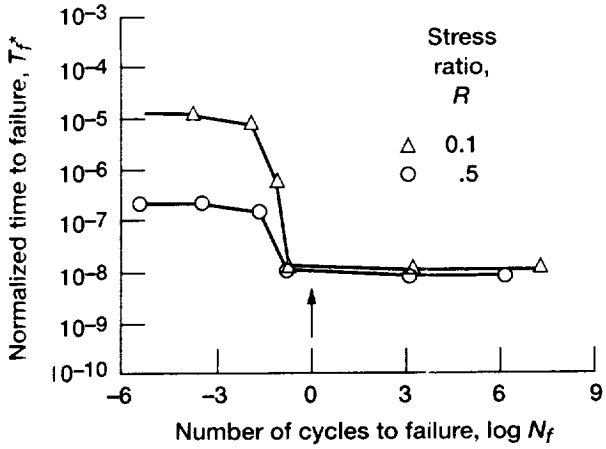

Figure 10.—Normalized time to failure T_f^* as function of number of cycles to failure N_f in cyclic (sinusoidal) stress loading for R-ratios of 0.1 and 0.5 under for $n = 20$ and $\sigma^*_{max} = 0.9$. Arrow indicates number of cycles corresponding to unity.

where $\omega a_i/A$ is the input value for numerical procedures, as shown in equation (17). As seen from figure 10, T_f^* decreases rapidly around $N_f = 10^{-1}$ to 10^0 and thereafter approaches a plateau that corresponds to the exact solution of time to failure. In other words, as long as the total number of cycles to failure is ≥1, the solution of time to failure is converged and is thus independent of either the number of cycles or frequency. Hence in the numerical procedure, the value of $\omega a_i/A$ was chosen to fulfill this requirement and started with a minimum value of 10^8, depending on T_f^*. This frequency independency in the exponential formulation is the same as that in the power-law formulation (refs. 5 and 17). For the power-law formulation, the time to failure remains unchanged with frequency, which is attributed to the functional form of $(1/\tau)\int_0^\tau [f(t)]^n dt$ in equation (7) (ref. 5). It can be easily shown that the period τ of any applied loading cycle is always cancelled out in the formulation. It should be noted that in this analysis, the presence of another damage mechanism (refs. 19 to 21) in addition to slow crack growth was not assumed to occur in cyclic loading. Only slow crack growth was considered as the unique mechanism leading to the failure of a material.

Comparison of Constant Stress and Cyclic Stress Loading Lifetimes: the h-Ratio

The ratio of constant stress and cyclic stress loading lifetimes, the h-ratio, with a condition of σ^* in constant stress loading equal to σ^*_{max} in cyclic stress loading ($\sigma^* = \sigma^*_{max}$), has been frequently used in the power-law formulation (refs. 5, 17, and 18) to quickly compare lifetimes of constant stress and cyclic stress loading. As done customarily for the power-law formulation, the h-ratio was also calculated for the exponential formulation. The h-ratio is defined as (refs. 5, 17, and 18)

$$h = \frac{t_{fs}}{t_{fc}} \tag{39}$$

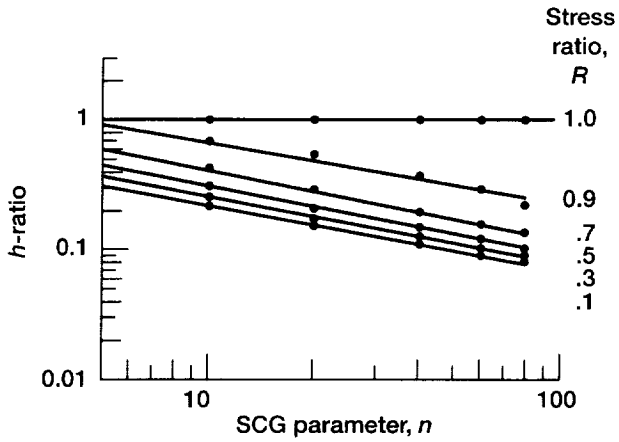

Figure 11.—Ratio of constant stress to cyclic stress loading lifetimes, h-ratio, as function of SCG parameter n for different R-ratios in cyclic (sinusoidal, $\sigma^*_{max} = 0.7$) loading. Each line represents best fit.

where again t_{fs} and t_{fc} are times to failure in constant stress and cyclic stress loading, respectively. Based on the numerical results of time to failure for constant stress and cyclic stress loading, the h-ratio was calculated using equation (39), and the results are presented in figure 11 as a function of n for different values of the R-ratio. The h-ratio decreases with increasing n, and the rate of decrease with increasing n is almost the same regardless of R-ratio up to 0.9. Also, for a given n, the h-ratio increases with increasing R-ratio. Note that the R-ratio of 1.0 represents the case for constant stress loading so that when $R = 1.0$, the numerical solution in cyclic stress loading should reduce to the case of constant stress loading. This presents another way to check the accuracy of the cyclic stress loading analysis. The h-ratio varies slightly by a factor of 2 between $\sigma^*_{max} = 0.2$ and 0.9: the lower σ^*_{max} value gives the higher h-ratio and vice versa. Hence, for a conservative estimate, the higher value of $\sigma^*_{max} = 0.7$ was used for the calculation of the h-ratio. The maximum difference in life between cyclic stress and constant stress loading is approximately 1 order of magnitude, which occurs for $R = 0.1$ and $n \geq 80$. A similar trend in the h-ratio can also be observed in the power-law formulation, as shown in figure 12. Here the plots of the h-ratio as a function of n are shown for a range of $R = 0.0$ to 1.0, calculated previously for the power-law formulation (ref. 17). Unlike the exponential formulation, no effect of σ^*_{max} on the h-ratio for a given R-ratio had been observed for the power-law formulation. Although no significant difference exists in the plots of h-ratio versus n between the exponential (fig. 11) and power-law (fig. 12) formulations, the overall magnitude of the h-ratio is about 20 percent greater in the exponential than in the power-law formulation.

Other Exponential Formulations

A comparison of solutions from other exponential SCG formulations under three loading configurations is shown in figure 13. The figure presents the results of three exponential formulations of equations (9) to (11) for $n = 20$ and 40 and compares them with those of the primary formulation of equation (8). The difference in solution between this primary equation and two other equations ((9) and (10)) was insignificant, particularly at higher stress rates (in constant stress rate loading, fig. 13(a)) and higher applied stresses (in constant stress and cyclic stress loading, figs. 13(b) and (c)), giving rise to a reasonable linearity between the dependent/independent variables related. This insignificant difference in solution as well as the linearity allows one to conclude that the primary equation would be representative of all three exponential SCG formulations considered. By contrast, the remaining second-order formulation

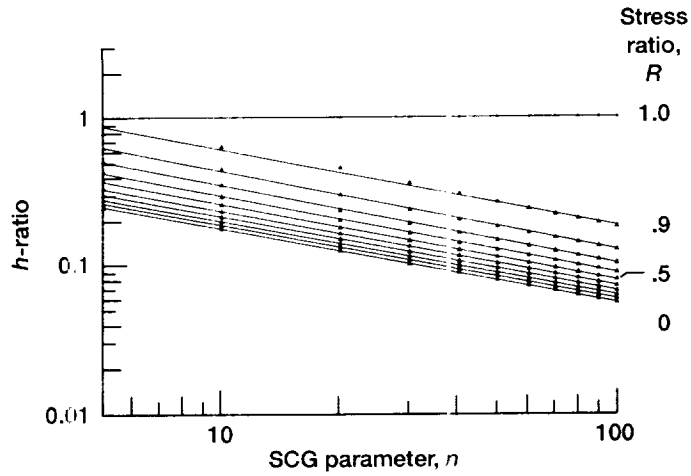

Figure 12.—Ratio of constant stress to cyclic stress loading lifetimes, h-ratio, as function of SCG parameter n for different R-ratios in cyclic (sinusoidal) stress loading, calculated with power-law formulation (ref. 17). Each line represents best fit.

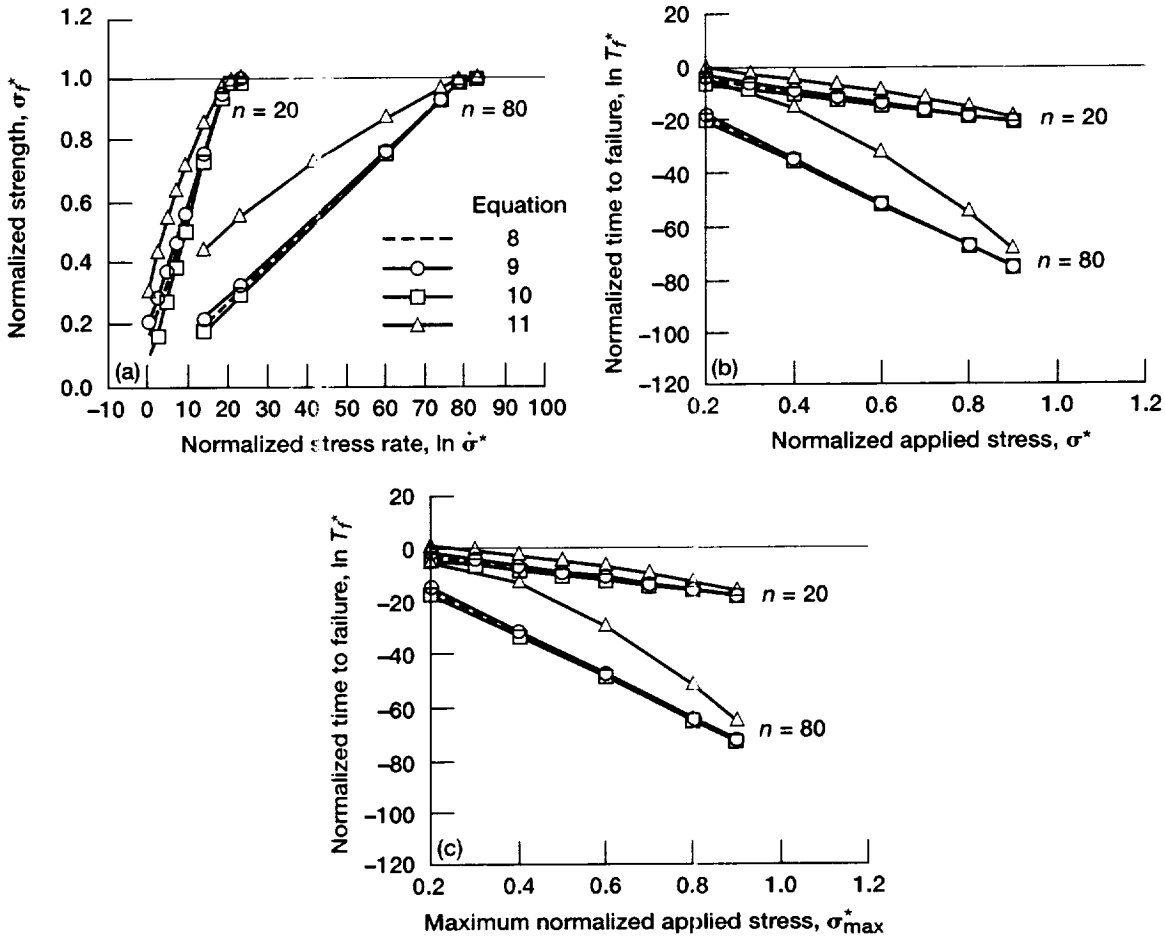

Figure 13.—Results of numerical solutions using three exponential formulations of equations (9) to (11) compared with the primary exponential formulation of equation (8) for selected SCG parameters of n = 20 and 80. (a) Constant stress-rate loading. (b) Constant stress loading. (c) Cyclic stress loading with stress ratio R = 0.1.

(eq. (11)) showed an appreciable deviation and a notable nonlinearity. Therefore, the determination of corresponding SCG parameters in this case differs from that of the primary equation and should only be attempted under appropriate circumstances so that a simple linear regression could be applied with reasonable accuracy. It is expected that considering its functional form, equation (12) also would yield results similar to those of equation (11).

Although the use of the exponential formulations to determine the SCG parameters of a material requires somewhat inconvenient numerical procedures, the resulting solutions given in this report would have almost the same degree of simplicity in both data analysis and experiments as the power-law formulation in constant stress rate, constant stress, or cyclic stress loading configurations. However, the knowledge of inert strength of a material should be known beforehand so that the corresponding SCG parameters (particularly n) can be determined, which could be a major drawback of the exponential formulation. In parts 2 and 3 of this report series, a variety of experimental data from various glasses and advanced ceramics at both ambient and elevated temperatures will be used to verify the solutions given herein.

Conclusions

Based on the numerical solutions of life prediction parameters obtained with exponential formulations, the following conclusions were made:

1. In constant stress rate (dynamic fatigue) loading, slow-crack-growth (SCG) parameters can be determined by a linear regression analysis of the data of (fracture stress/inert strength) as a function of applied stress rate, σ_f/S_i versus $\ln \dot{\sigma}$, together with the appropriate relations provided.

2. In constant stress (static fatigue or stress rupture) and cyclic stress (cyclic fatigue) loading, the corresponding SCG parameters can be evaluated by a linear regression analysis of the data of time to failure as a function of (maximum applied stress/inert strength), $\ln t_f$ versus σ_{max}/S_i, in conjunction with the pertinent relations provided.

3. No frequency effect on life and no dependency of SCG parameter n on the R-ratio, the ratio of minimum to maximum applied stress, was observed in cyclic stress loading, much the same as that observed for the power-law formulation. The difference in the ratio of constant stress to cyclic stress loading lifetimes, the h-ratio, between the exponential and power-law formulations was minimal with a maximum difference of about 20 percent.

4. While the numerical solutions using the exponential formulation require somewhat inconvenient numerical procedures, they provide almost the same level of simplicity in both data analysis and experiments as the power-law formulation. However, requiring the knowledge of the inert strength of a material to determine corresponding SCG parameters (particularly n) would make the exponential formulation more difficult to use in comparison with the power-law formulation.

5. There is no appreciable difference in solutions between the primary exponential SCG equation (used in this analysis) and two other exponential expressions analyzed in this study, so the primary equation would be considered representative of all the first-order exponential formulations.

Appendix—Symbols

A	slow-crack-growth parameter defined in equations (1) and (8)
a	crack size
B	slow-crack-growth parameter, $B = 2K_{IC} / [AY^2(n-2)]$
C	crack size in normalized scheme of references 15 to 17
D	slow-crack-growth parameter defined in equations (5) to (7)
$f(t)$	periodic function, cyclic loading
h	ratio of constant to cyclic stress loading lifetimes
K	stress intensity factor
N	number of cycles
n	slow-crack-growth parameter defined in equations (1) and (8)
R	stress ratio
r^2	correlation coefficient
S	strength
T	time in normalized scheme of references 15 to 17
t	time
v	crack velocity
Y	crack geometry factor
β	intercept of curve in linear regression analysis defined in equations (18), (26), and (32)
χ	slow-crack-growth parameter defined in equations (23), (31), and (37)
σ	applied stress
$\dot{\sigma}$	applied stress rate
τ	period
ω	angular velocity

Subscripts:

C	critical
c	cyclic stress
d	constant stress rate
f	fracture
I	mode I
i	inert or initial condition
max	maximum
min	minimum
s	constant stress

Superscripts:

*	normalized
′	apparent (calculated)

References

1. Standard Test Method for Determination of Slow Crack Growth Parameters of Advanced Ceramics by Constant Stress-Rate Flexural Testing at Ambient Temperature. Annual Book of ASTM Standards 2000, ASTM Designation: C 1368–00, sec. 15, vol. 15.01, ASTM, West Conshohocken, PA, 2001, pp. 626–634.
2. Standard Test Method for Determination of Slow Crack Growth Parameters of Advanced Ceramics by Constant Stress-Rate Flexural Testing at Elevated Temperatures. Annual Book of ASTM Standards 2001, ASTM Designation: C 1465–00, sec. 15, vol. 15.01, ASTM, West Conshohocken, PA, 2001, pp. 703–716.
3. Wiederhorn, S.M.: Subcritical Crack Growth in Ceramics. Fracture Mechanics of Ceramics, R.C. Bradt, D.P.H. Hasselman, and F.F. Lange, eds., vol. 2, Plenum Press, New York, NY, 1974, pp. 613–646.
4. Ritter, John E., Jr.: Engineering Design and Fatigue Failure of Brittle Materials. Fracture Mechanics of Ceramics, R.C. Bradt, D.P.H. Hasselman, and F.F. Lange, eds., vol. 4, Plenum Press, New York, NY, 1978, pp. 667–686.
5. Evans, A.G.; and Fuller, E.R.: Crack Propagation in Ceramic Materials Under Cyclic Loading Conditions. Metall. Trans., vol. 5, no. 1, 1974, pp. 27–33.
6. Hillig, W.B.; and Charles, R.J.: Surfaces, Stress-Dependent Surface Reactions, and Strength. High-Strength Materials, Victor F. Zackay, ed., ch. 17, John Wiley & Sons, Inc., New York, NY, 1965, pp. 682–705.
7. Charles, R.J.: Diffusion Controlled Stress Rupture of Polycrystalline Materials. Metall. Trans. A, vol. 7A, no. 8, 1976, pp. 1081–1089.
8. Pollet, J.-C.; and Burns, S.J.: Thermally Activated Crack Propagation—Theory. Int. J. Fracture, vol. 13, no. 5, 1977, pp. 667–679.
9. Wiederhorn, S.M.; and Bolz, L.H.: Stress Corrosion and Static Fatigue of Glass. J. Am. Ceram. Soc., vol. 53, no. 10, 1970, pp. 543–548.
10. Lawn, B.R.: An Atomistic Model of Kinetic Crack Growth in Brittle Solids. J. Mater. Sci., vol. 10, 1975, pp. 469–480.
11. Lenoe, E.M.; and Neal, D.M.: Assessment of Strength-Probability-Time Relationships in Ceramics. ARPA Order 2181, AMMRC–TR–75–13, 1975.
12. Trantina, G.G.: Strength and Life Prediction for Hot-Pressed Silicon Nitride. J. Am. Cer. Soc., vol. 62, no. 7–8, 1979, pp. 377–380.
13. Ritter, John E., et al.: Dynamic Fatigue Analysis of Indentation Flaws Using an Exponential-Law Crack Velocity Function. Commun. Am. Ceram. Soc., 1984, pp. C–198—C–199.
14. Ritter, John E., Jr.; Jakus, Karl; and Cooke, David S.: Predicting Failure of Optical Glass Fibers. Environmental Degradation of Engineering Materials in Aggressive Environments, Proceedings of Second International Conference on Environmental Degradation of Engineering Materials, 1981, pp. 565–575.
15. Lawn, B.R., et al.: Fatigue Analysis of Brittle Materials Using Indentation Flaws. J. Mat. Sci., pt. 1, vol. 16, 1981, pp. 2846–2854.
16. Choi, S.R.; Ritter, J.E.; and Jakus, K.: Failure of Glass With Subthreshold Flaws. J. Am. Ceram. Soc., vol. 73, no. 2, 1990, pp. 268–274.
17. Choi, Sung R.; and Salem, Jonathan A.: Cyclic Fatigue of Brittle Materials With an Indentation-Induced Flaw System. Mater. Sci. Eng., vol. A208, no. 1, 1996, pp. 126–130.

18. Kawakubo, Takashi; and Komeya, K.: Static and Cyclic Fatigue Behavior of a Sintered Silicon Nitride at Room Temperature. J. Am. Ceram. Soc., vol. 70, no. 6, 1987, pp. 400–405.
19. Horibe, S.; and Hirahara, R.: Cyclic Fatigue of Ceramic Materials: Influence of Crack Path and Fatigue Mechanisms. Acta. Metall. Mater., vol. 39, no. 6, 1991, pp. 1309–1317.
20. Ewart, L.; and Suresh, S.: Crack Propagation in Ceramics Under Cyclic Loads. J. Mater. Sci., vol. 22, no. 4, 1987, pp. 1173–1192.
21. Dauskardt, Reinhold H.; Marshall, David B.; and Ritchie, Robert O.: Cyclic Fatigue-Crack Propagation in Magnesia-Partially-Stabilized Zirconia Ceramics. J. Am. Ceram. Soc., vol. 73, no. 4, 1990, pp. 893–903.

REPORT DOCUMENTATION PAGE

Form Approved
OMB No. 0704-0188

1. AGENCY USE ONLY (*Leave blank*)	2. REPORT DATE	3. REPORT TYPE AND DATES COVERED
	June 2002	Technical Memorandum

4. TITLE AND SUBTITLE

Slow Crack Growth of Brittle Materials With Exponential Crack-Velocity Formulation—Part 1: Analysis

5. FUNDING NUMBERS

WU–708–31–13–00

6. AUTHOR(S)

Sung R. Choi, Noel N. Nemeth, and John P. Gyekenyesi

7. PERFORMING ORGANIZATION NAME(S) AND ADDRESS(ES)

National Aeronautics and Space Administration
John H. Glenn Research Center at Lewis Field
Cleveland, Ohio 44135–3191

8. PERFORMING ORGANIZATION REPORT NUMBER

E–13009–1

9. SPONSORING/MONITORING AGENCY NAME(S) AND ADDRESS(ES)

National Aeronautics and Space Administration
Washington, DC 20546–0001

10. SPONSORING/MONITORING AGENCY REPORT NUMBER

NASA TM—2002-211153-PART1

11. SUPPLEMENTARY NOTES

Sung R. Choi, Ohio Aerospace Institute, Brook Park, Ohio 44142; Noel N. Nemeth and John P. Gyekenyesi, NASA Glenn Research Center. Responsible person, Sung R. Choi, organization code 5920, 216–433-8366.

12a. DISTRIBUTION/AVAILABILITY STATEMENT

Unclassified - Unlimited
Subject Categories: 07 and 39 Distribution: Nonstandard

Available electronically at http://gltrs.grc.nasa.gov/GLTRS

This publication is available from the NASA Center for AeroSpace Information, 301–621–0390.

12b. DISTRIBUTION CODE

13. ABSTRACT ***(Maximum 200 words)***

Extensive slow-crack-growth (SCG) analysis was made using a primary exponential crack-velocity formulation under three widely used load configurations: constant stress rate, constant stress, and cyclic stress. Although the use of the exponential formulation in determining SCG parameters of a material requires somewhat inconvenient numerical procedures, the resulting solutions presented gave almost the same degree of simplicity in both data analysis and experiments as did the power-law formulation. However, the fact that the inert strength of a material should be known in advance to determine the corresponding SCG parameters was a major drawback of the exponential formulation as compared with the power-law formulation.

14. SUBJECT TERMS

Slow crack growth analysis; Life prediction; Brittle materials; Ceramics and glass; Life prediction testing; Mechanical testing

15. NUMBER OF PAGES

26

16. PRICE CODE

17. SECURITY CLASSIFICATION OF REPORT	18. SECURITY CLASSIFICATION OF THIS PAGE	19. SECURITY CLASSIFICATION OF ABSTRACT	20. LIMITATION OF ABSTRACT
Unclassified	Unclassified	Unclassified	